Journal of Peptide Science, Vol. 1, 330–340 (1995)

Conformational Behaviour of a Cyclolinopeptide A Analogue: Two-dimensional NMR study of cyclo(Pro[1]-Pro-Phe-Phe-Ac_6c-Ile-ala-Val[8])

MARCO MAZZEO[1], CARLA ISERNIA[2], FILOMENA ROSSI[1], MICHELE SAVIANO[1], CARLO PEDONE[1], LIVIO PAOLILLO[1], ETTORE BENEDETTI[1] and VINCENZO PAVONE[1]

[1]Centro di Studio di Biocristallografia del C.N.R., Dipartimento di Chimica, Università di Napoli, Napoli, Italy
[2]Facoltà di Scienze Ambientali, Seconda Università di Napoli, Caserta, Italy

Received 6 April 1995
Accepted 19 May 1995

Abstract: The cyclic octapeptide cyclo[-Pro[1]-Pro-Phe-Phe-Ac_6c-Ile-ala-Val[8]-] [C_8-Ac_6c], containing the Pro[1]-Pro-Phe-Phe sequence, followed by a bulky helicogenic $C^{\alpha,\alpha}$-dialkylated glycine residue Ac_6c (1-aminocyclohexane-1-carboxylic acid), and a D-Ala residue at position 7 has been synthesized. This cyclic peptide is a deletion analogue of the naturally occurring cyclic nonapeptide cyclolinopeptide A (CLA). It has been designed with the aim of studying the role that the Ac_6c and D-Ala residues play on the conformational behaviour of the whole molecule and their influence on the conformation of the Pro[1]-Pro-Phe-Phe sequence when compared with cyclolinopeptide A.

C_8-Ac_6c has been investigated in chloroform and acetonitrile solutions by 2D NMR techniques. Only one set of sharp signals is observed in both solvents. This evidence strongly supports the hypothesis that only one conformational state exists in the chosen solvents. The interpretation of the experimental data points to the existence for C_8-Ac_6c of a very rigid structure stabilized by intramolecular hydrogen bonds. The measured NOE effects allow the calculation of internuclear distances, which have been used as restraints in molecular dynamic calculations. The proposed conformation of the molecule shows that the Pro-Pro-Phe segment retains the conformation observed in natural CLA both in solution and in the solid state and that the Ac_6c residue indeed reinforces the ring rigidity not permitting the formation of any appropriate cavity in which inorganic cations could be complexed.

Keywords: Cyclolinopeptide A; cyclooctapeptides; NMR; conformational studies; restrained molecular dynamics

INTRODUCTION

The study of the influence of both ring skeleton reduction and of bulky amino acid substitution in a closely related series of cyclic peptides represents a powerful way of investigating conformational properties and structure–activity relationships.

In our laboratories a series of various cyclic compounds related to cyclolinopeptide A (CLA), a cyclic nonapeptide from linseed, has been synthesized in order to elucidate the dependence of the biological activity upon sequence and conformational behaviour of these peptides [1–13].

Our studies suggest that CLA and its cyclopeptide analogues exhibit high conformational mobility leading to the presence of a mixture of several conformers in solution at room temperature, with the exception of [Aib[5,6]-ala[8]]-cyclolinopeptide A (CLAIB) [6, 8, 11]. In fact, the conformational behaviour of this compound in solution indicates that, even at room temperature, the peptide remains conformationally homogenous and that its proposed structure is almost identical to that observed in the solid state. The solution conformational analysis reveals also

Address for correspondence: Prof. Ettore Benedetti, Dipartimento di Chimica, Università di Napoli, via Mezzocannone 4, I-80134, Napoli, Italy.

CCC 1075-2617/95/050330-11

that the constraints imposed by two consecutive Aib at positions 5 and 6 and D-Ala[8] residues are particularly strong. In fact, the conformational parameters are only slightly affected by large temperature variations and by the addition of salts [6]. The examination of the CLA and CLAIB structural parameters in solution and in the solid state [3, 6] proved that both compounds are characterized by the same backbone conformation with identical intramolecular hydrogen bond pattern. Particularly, they are characterized by two different chain reversals: (i) a C_{13} ring structure occurs between the Phe[4]NH and the Val[9] C'O containing the *cis* peptide unit; and (ii) a C_{16} ring structure between the Val[9] NH and Phe[4]C'O.

These turns are located on opposite sides of the cyclic structure and they contain residues at the Phe[4] and Val[9] border. These latter residues are in about semi-extended conformation and they face each other similarly to hydrogen bonded residues in an anti-parallel β-sheet arrangement. In the light of these observations we wanted to verify whether the reduction of the ring size (by the deletion of one residue in the CLA or CLAIB Phe[4]-Val[9] segment) could lead to an unmodified structure for the Pro[1]-Phe[4] region. Des-[Ile[6]] CLAIB would be a possible analogue; the Ac$_6$c residue was also chosen as a residue for its considerable lipophilicity [14], instead of the Aib residue.

A limited number of conformational studies of cyclooctapeptides are reported in the literature and in almost all cases they concern chemically and structurally symmetrical compounds [15–22]. Recently, Kessler and coworkers have reported the synthesis and conformational analysis of hymenistatin 1, a non-symmetrical cyclooctapeptide, characterized by biological activity similar to that of natural hymenistatin [23].

In the present paper we report the synthesis and the conformational analysis of cyclo(Pro-Pro-Phe-Phe-Ac$_6$c-Ile-ala-Val) carried out at room temperature by 2D NMR technique in different solvents and by restrained molecular dynamic simulations.

MATERIALS AND METHODS

Synthesis and Characterization

The synthesis of the linear octapeptide H-ala-Val-Pro-Pro-Phe-Phe-Ac$_6$c-Ile-OH was achieved by solid-phase methods with *t*-Boc protected amino acids using a 430A Applied Biosystem automatic synthesizer. This linear sequence was chosen on the basis of CLA conformational parameters in solution and in the solid state [3]. These data, in fact, suggested that the peptide chain could fold properly at the Pro-Pro segment and Ac$_6$c residue to bring D-Ala and Ile residues at close distance, thus favouring the cyclization step. Beside this, it seemed to us that D-Ala and Ile residues would provide a limited steric hindrance when related to other possible cyclization positions.

t-Boc-Ac$_6$c-OH was prepared according to a known procedure [24]; *N,N'*-dicyclohexylcarbodiimide (DCC) and 1-hydroxybenzotriazole (HOBt) were used as coupling reagents following standard procedures. *t*-Boc-Ac$_6$c-OH was dissolved in CH_2Cl_2 and coupled as an asymmetric anhydride twice in double excess. After release of the linear peptide from the resin by HF [25], the crude peptide was extracted from the resin with acetic acid, concentrated, diluted with water and lyophilized to give 325 mg of crude peptide (yield 90%). The crude peptide was purified by preparative HPLC using a Delta Prep 3000 Millipore-Waters system on a Vydac C18 (2.2 × 25 cm) column with a linear gradient H_2O 0.1% TFA: CH_3CN 0.1% TFA (yield 85%). FAB mass ($MH^+ = 915$) and amino acid analysis with chirality detection [26] were also performed.

Peptide cyclization was obtained in a diluted solution of DMF/CH_2Cl_2 (1:1 v/v) in the presence of isobutylchloroformate and *N*-methylmorpholine, pH = 8.2 at −10°C for 1 h. The reaction mixture, left overnight at room temperature, was then reduced in volume, diluted with water, extracted several times with $CHCl_3$, dried over Na_2SO_4 and evaporated *in vacuo*. The purification by preparative HPLC was carried out by a linear gradient H_2O 0.1% TFA: CH_3CN 0.1% TFA, and gave the pure cyclopeptide (yield 73%). FAB mass for MH^+ was 897, as expected. The amino acid analysis was performed by HPLC techniques with the Marfey's reagent derivatives as chiral agent [26] for the hydrolised samples. The Nucleosil C_{18} (100–107 μm) column at 30°C was eluted at 2 ml/min flow rate with a linear gradient of (A) 50 mM tetraethylammonium phosphate at pH = 3; (B): 50% CH_3CN in A; detection at 340 nm. The amino acidic composition was: L-Pro 2.0; L-Phe 2.0; L-Ile 0.91; D-Ala 0.89; L-Val 1.0; the Ac$_6$c peak intensity was weak and undetected.

NMR Measurements

NMR data were collected on a VARIAN UNITY 400 MHz spectrometer equipped with a SUN compu-

ter SPARC 330 and processed on a SUN SPARC Station 1+.

All ^1H spectra were recorded at 298 K and referenced to internal TMS. NMR samples were prepared by dissolving 2.2 mg of peptide either in 0.75 ml of CD_3CN (99.96% ^2H atom, Cambridge Isotope Laboratories) or in 0.75 ml of $CDCl_3$ (99.96% ^2H atom, Aldrich). An additional very diluted solution was prepared by dissolving 0.22 mg of peptide in 0.75 ml of both solvents. Concentrated solutions at 16 mg in 0.75 ml of both solvents were used for monodimensional ^{13}C, HMQC and HMBC experiments.

One-dimensional experiments have been typically acquired using 64–128 scans with 32 K data points. The spectra for the determination of the temperature coefficients were recorded at 298–318 K in steps of 5 K.

Deuterium isotope exchange was simply followed in both solvent systems by adding excess amounts of D_2O into the NMR tube and measuring the amide proton area loss with time.

Phase-sensitive double quantum filtered correlated spectroscopy (DQFCOSY) [27], homonuclear Hartmann–Hahn (Clean TOCSY) [28] and nuclear Overhauser effect spectroscopy in the laboratory and in the rotating frames (NOESY, ROESY) [29, 30] were performed according to the States–Haberkorn method and applying standard phase cycling schemes. Off-resonance effects were compensated with two 90° hard pulses before and after the spin lock period [31].

These experiments were typically acquired with 256 increments and 2048 data points in t_2 and zero filled to 1 K in F_1. Mixing time values were 70 ms for TOCSY, in the range 50–400 ms for NOESY and in the range 30–200 ms for ROESY spectra.

NOESY and ROESY cross-peak intensities were evaluated by volume integration using the available VARIAN software.

Inverse heteronuclear multiple quantum correlation (HMQC, HMBC) [32, 33] spectroscopy was used to assign ^{13}C resonances. 256 t_1 increments with 192 transients of 2048 points were acquired with the States–Haberkorn method. HMQC was recorded with a BIRD nulling τ delay equal to 300 ms.

For selective excitation in the TOCSY-1D [34] experiments a TOPHAT shaped pulse of 175 ms was used.

Restrained Molecular Dynamics

RMD simulations were carried out on a Silicon Graphics (Personal Iris 4D35 GT Turbo) workstation employing the INSIGHT/DISCOVER program [35]. The consistent valence force field (CVFF) was utilized for all simulations [36–38]. The equations of motion were solved using the so-called Leapfrog integration algorithm [39].

NMR NOE contacts were sufficient to build a reasonable starting model of the cyclic compound for the Restrained Molecular Dynamics (RMD) cycles. A hundred steps of energy minimizations to eliminate hot spots [40] using the conjugate gradient method [40] were performed for the starting structure. The energy-minimized structure was used as the initial structure for the RMD *in vacuo* at 300 K. All unambiguous NOE effects were used for the MD calculations. In each RMD simulation, performed with a time step of 0.5 fs, the molecule was equilibrated for 60 ps. After this first step, an additional 80 ps of simulation without rescaling was carried out since energy conservation was observed and the average temperature remained essentially constant around the target value of 300 K.

The final structure was then checked for consistency with all observable NOE. Coordinates and velocities for the simulation were dumped to a disk every 10 steps during the last 20 ps of the simulations. The dumped data were used for the statistical analysis.

RESULTS AND DISCUSSION

NMR

The structural behaviour of cyclo{Pro^1-Pro-Phe-Phe-Ac_6c-Ile-ala-Val^8} has been studied in two different solvent media, chloroform and acetonitrile.

The ^1H 1D spectrum in both solvent systems (Figure 1) shows one set of sharp signals in a wide range of temperatures. This evidence strongly suggests that only one conformer is present in solution. The assignment of all spin systems was carried out using conventional [41] TOCSY and DQFCOSY spectra. ^{13}C spectra have been assigned with the aid of HMQC and HMBC experiments. In chloroform solution the proton spectrum shows overlaps of the Pro^2 αCH signal with the Pro^1 δ'CH signals (3.64 p.p.m.) and of the Pro^1 αCH with the Pro^2 δ'CH signals (3.18 p.p.m.). The unambiguous assignments of these resonances are, on the other hand, essential for the stereochemical characterization around the two proline residues of the cyclic molecule. This problem has been solved by an heteronuclear HMBC

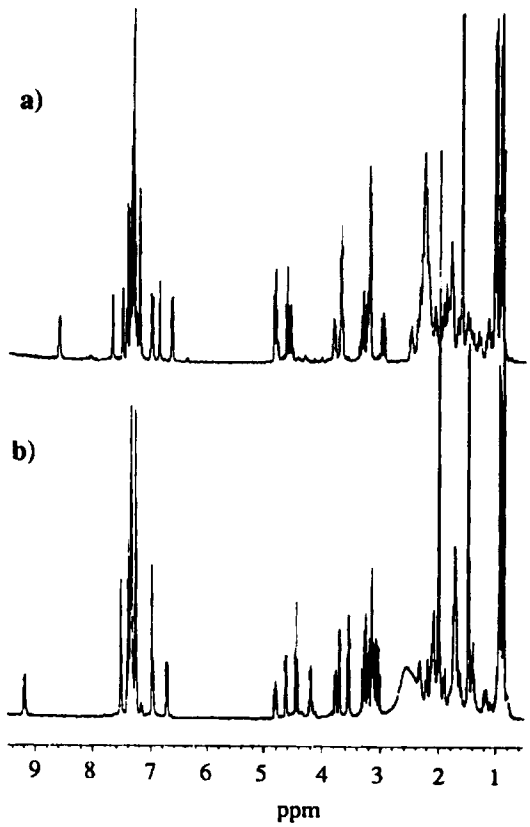

Figure 1 Monodimensional spectra in $CDCl_3$(a) and in CD_3CN (b) at 298 K.

2D experiment in the reverse mode. In Figure 2 two regions of the HMBC map, showing the correlations between the Pro^2 CO and the nearby NH and αCH protons, are presented. The long-range correlations 171.3–8.61 p.p.m. and 171.3–3.64 p.p.m. are assigned respectively to COPro^2–NHPhe^3 and COPro^2–αCHPro^2 resonances. Thus the specific proton assignment to the two proline residues can be made. Selective 1D-TOCSY experiments were further acquired to confirm the assignment. Sequential assignments were typically obtained from the NOESY and ROESY 2D spectra using the well-known α-CH_i–NH_{i+1} and NH_i-NH_{i+1} backbone interactions.

Proton and carbon chemical shifts, in the two solvents, are reported in Tables 1 and 2, respectively. The values appear quite similar in both solvents and similar to those reported for CLA [3] and CLAIB [6]. No changes in the 0.33, 3.3 and 24 mM range were observed for all chemical shifts. The Pro^2-γ' proton experiences a consistent high-field shift, as already found for CLA and CLAIB, while the Phe^3 NH exhibits a marked distinct chemical shift accounted for by a different effect of the Phe^3 ring current.

The configuration around the two proline residues was assigned from the chemical shift difference between proline β and γ carbon resonances as can be observed in the HMQC 2D map in $CDCl_3$ shown in Figure 3. In both solvents this difference amounts to 3.5 and 9.8 p.p.m. for Pro^1 and Pro^2, respectively.

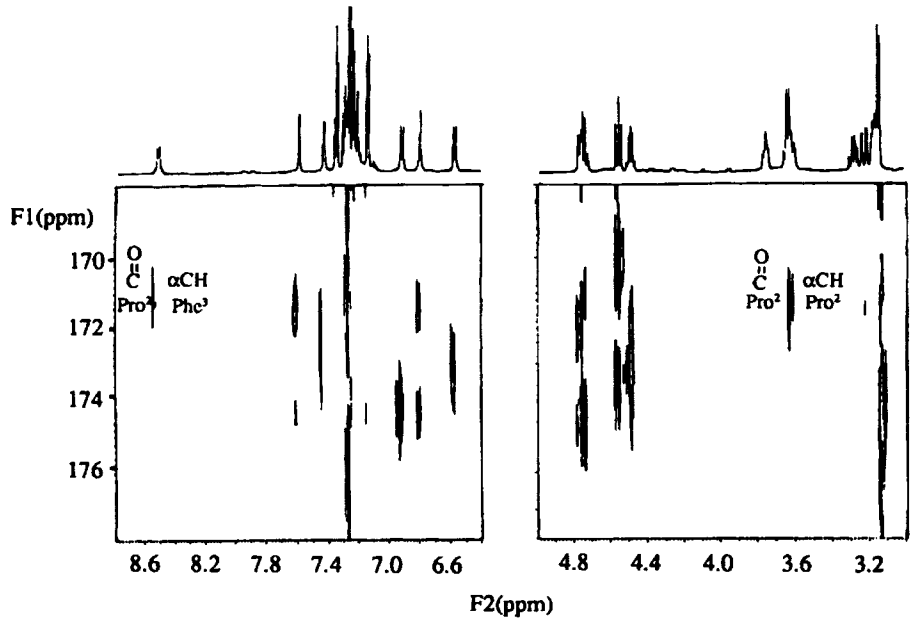

Figure 2 Regions of the HMBCR spectrum in $CDCl_3$ showing CO–NH and CO–αCH correlations.

Table 1. Proton Chemical Shifts (p.p.m.) at 298 K

Residue	NH	αCH	βCH	γCH	Others
CD_3CN					
Pro^1		3.21	2.00(S)–1.70(R)	2.10–1.70	δδ′CH 3.54
Pro^2		3.70	2.11(R)–1.97(S)	1.62–0.80	δδ′CH 3.27–3.13
Phe^3	9.19	4.81	3.29(S)–3.13(R)		(2,6)H 7.28; (3,4,5)H 7.34
Phe^4	7.53	3.77	3.17(S)–3.05(R)		(2,6)H 7.34; (3,4,5)H 7.40
Ac_6c^5	6.99		1.92–1.72	1.72–1.44	1.72–1.39
			2.19–2.13	1.78–1.42	
Ile^6	6.97	4.62	2.33	1.48–1.18	0.87γCH_3; 0.87δCH_3
ala^7	7.53	4.19	1.48		
Val^8	6.71	4.44	2.07	0.91–0.95	
$CDCl_3$					
Pro^1		3.18	1.87(S)–1.75(R)	2.13–1.75	δδ′CH 3.64–3.54
Pro^2		3.65	2.23(R)–1.90(S)	1.63–0.82	δδ′CH 3.29–3.18
Phe^3	8.61	4.76	3.14		(2,6)H 7.13; (3,5)H 7.30; (4)H 7.21
Phe^4	7.56	3.64	3.23(S)–2.88(R)		(2,6)H 7.26; (3,5)H 7.38; (4)H 7.33
Ac_6c^5	6.69		1.83–1.54	1.80–1.43	1.70–1.34
			2.28–2.17	1.76–1.24	
Ile^6	6.97	4.79	2.42	1.41–1.09	0.84γCH_3; 0.88δCH_3
ala^7	7.49	4.51	1.55		
Val^8	6.65	4.56	2.00	0.97–0.94	

Table 2 ^{13}C Chemical Shift (p.p.m.) at 298 K

Residue	CO	αC	βC	γC	δC
CD_3CN					
Pro^1		59.3	28.8	25.2	47.2
Pro^2		60.9	30.9	21.1	46.4
Phe^3		52.4	33.3		
Phe^4		60.6	36.6		
Ac_6c^5		60.1	35.4–28.8	21.1–21.3	25.0
Ile^6		57.1	36.3	24.7; γCH_3 15.1	11.4
ala^7		50.2	17.4		
Val^8		55.8	28.8	18.8–17.5	
$CDCl_3$					
Pro^1	170.0	58.7	28.7	25.3	47.5
Pro^2	171.4	60.8	31.3	21.2	46.8
Phe^3	174.3	52.9	34.4		
Phe^4	171.2	61.3	37.0		
Ac_6c^5	174.3	60.0	35.9–28.5	21.8–21.2	24.9
Ile^6	172.3	57.5	35.9	24.9; γCH_3 15.7	12.0
ala^7	173.5	50.2	17.4		
Val^8	170.2	55.8	31.4	19.3–17.6	

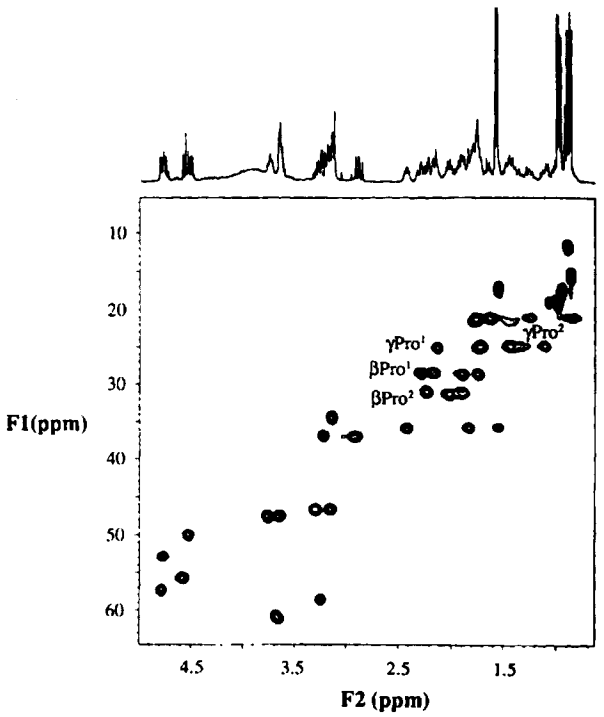

Figure 3 High-field region of the HMQCR spectrum in $CDCl_3$ at 298 K.

Thus we can conclude that the Val^8-Pro^1 and the Pro^1-Pro^2 peptide bonds are in the *trans* and *cis* conformations, respectively. These conclusions were further confirmed by NOE contacts between the αCHVal^8-δCHPro^1 and between the αCHPro^1–αCHPro^2 protons. This latter contact, in principle, could also be due to α and δ protons within the same proline residue (see Table 1) but this is to be excluded on the simple structural grounds that the two protons are not closer than 4 Å.

$^3J_{NH-\alpha CH}$, $^3J_{\alpha CH-\beta CH}$ and $^3J_{\alpha CH-\beta' CH}$ coupling constants have been directly measured from the one-dimensional spectrum and confirmed in the DQFCOSY spectrum. It should be noted that the small $^3J_{NH-\alpha CH}$ value of Phe^4 is consistent with values of −50°, 0°, 120°, 170° for the conformational ϕ angle. Diastereotopic assignment was obtained on the basis of $^3J_{\alpha CH-\beta CH}$ and $^3J_{\alpha CH-\beta' CH}$ coupling constants and NH_i–$\beta,\beta' CH_i$ NOE effects. Furthermore, Phe^3 and Phe^4 sidechain orientations experience *gauche*(-) χ_1 angles.

Coupling constants and temperature coefficients of amide protons, measured in both solvents, are listed in Table 3. Low temperature coefficients were observed for the NH protons in the Phe^4-Val^8 segment (with the exception of Ac$_6$c), suggesting that these protons are solvent shielded [42]. Furthermore, no changes in the 0.33–3.3 mM range were observed for the amide temperature dependence chemical shifts, thus indicating the absence of aggregation phenomena in this concentration range.

In order to gain more information on the shielding of the amide NH protons, a deuterium exchange experiment was carried out in both solvents. The data obtained indicate that in both solvents the NH protons of Phe^4 and Ac$_6$c^5 exchange considerably faster than the others. For example in $CDCl_3$ solution the lifetimes for Phe^4 and Ac$_6$c^5 are around 10^2–10^3 seconds, whereas they are higher for all other NH protons. This behaviour clearly demonstrates that the low-temperature coefficient of Phe^4 cannot be taken as a sound proof of a hydrogen bond [43].

NOE effects were measured for structural purposes. Both NOESY and ROESY 2D experiments were carried out at various mixing times in order to evaluate cross-relaxation rates. From these, by applying the method described in [44], it is possible to estimate the interatomic distances. It is, however, important to underline that any of the methods currently used is based on two assumptions: that the molecule is structurally rigid and that it tumbles isotropically. These two assumptions were proved valid in our case. In fact, all NMR parameters such as coupling constants, temperature coefficients, T_1 relaxation times and NOE effects point to a rigid structure with intramolecular hydrogen bonds. Secondly, T_1 carbon relaxation times, measured in both solvents, demonstrate a large similarity of the αC values along the entire backbone (between 0.3–0.4 s in $CDCl_3$ and 0.6–0.7 s in CD_3CN), thus showing that, as far as the backbone is concerned, the molecule is within the isotropic motion limits.

Considering that the backbone correlation time τ_c is the same for all spin pairs, cross-relaxation rates were compared with those of γγ′ Pro^2 protons whose distance was taken as 1.78 Å. Calculated interatomic distances from NOESY and ROESY spectra appear very similar, only the main values obtained from NOESY are listed in Table IV. Unusual long-range Overhauser effects NH Phe^3-αCH Pro^1, αCH Phe^4-βCH_3 ala^7, (3,4,5)H Phe^4-β,γCH Pro^1 and (3,4,5)H Phe^3-β′CH Pro^2 were found.

Restrained Molecular Dynamics

The conformational behaviour of C8-Ac$_6$c was examined by RMD simulation. The analysis of NOE effects

Table 3 Temperature Coefficients (p.p.b./K), Coupling Constants (Hz) and Corresponding ϕ Dihedral Angles

Residue	$\Delta\delta/\Delta T$	$^3J_{NH\text{-}\alpha CH}$	ϕ	$^3J_{\alpha CH\text{-}\beta CH}$	$^3J_{\alpha CH\text{-}\beta' CH}$
CD_3CN					
Pro^1				0	8.3
Pro^2				8.3	0
Phe^3	−4.2	8.7	−1.40°, −100°	5.0	11.3
Phe^4	−1.0	3.1	−50°, 0°, 120°	3.1	10.9
Ac_6c^5	−1.4				
Ile^6	+1.2	10.2	−120°	3.4	
ala^7	−1.4	5.1	170°, 65°, −20°, −100°	7.4	
Val^8	−0.6	9.9	−120°	9.9	
$CDCl_3$					
Pro^1				0	8.2
Pro^2				7.9	0
Phe^3	−6.6	8.1	−150°, −90°		
Phe^4	0	2.0	−20°, 140°	2.7	11.2
Ac_6c^5	+2.6				
Ile^6	−1.0	10.2	−120°	3.5	
ala^7	−1.5	5.9	170°, 70°, −30°, −100°	7.6	
Val^8	−0.5	9.7	−120°	9.7	

Table 4 Interproton Distances (Å) Calculated from NOESY Spectra in CD_3CN and the average values during the RMD simulation[a]

Cross peak	d_n (Å)	*d*RMD (Å)
$NHala^7$–$NHVal^8$	2.6	2.9
$NHPhe^3$-$NHPhe^4$	4.3	**3.6**
$NHala^7$–$NHIle^6$	2.2	2.3
$NHPhe^3$-$\alpha CHPro^1$	2.5	**2.0**
$NHPhe^3$–$\alpha CHPhe^3$	3.0	3.1
$NHPhe^3$–$\beta CHPhe^3$	2.7	**2.7**
$NHPhe^3$–$\beta' CHPhe^3$	3.1	3.8
$NHPhe^4$–$\alpha CHPhe^3$	2.4	2.4
$NHPhe^4$–$\alpha CHPhe^4$	2.7	2.8
$NHPhe^4$-$\beta CHPhe^4$	3.3	3.5
$NHPhe^4$-$\beta' CHPhe^4$	2.7	2.5
$NHala^7$–αala^7	3.0	3.0
$NHala^7$–βCH_3ala^7	2.5	2.7
$NHala^7$–$\alpha CHIle^6$	3.2	3.4
$NHIle^6$–$\gamma\delta CH_3Ile^6$	2.9	3.0
$NHIle^6$–$\gamma CHIle^6$	3.1	3.0
$NHVal^8$–γCH_3Val^8	2.7	2.5
$NHVal^8$–$\gamma CHIle^6$	2.7	2.6
$\alpha CHPhe^4$–βCH_3ala^7	2.7	2.9
$\alpha CHVal^8$–$\delta CHPro^1$	2.2	2.2
$\beta CHVal^8$–$\delta CHPro^1$	2.4	2.5
$\alpha CHPro^1$–$\alpha CHPro^2$	2.1	2.5

[a]For the upper and lower distant restraint, 10% was added or subtracted. The distance restraints with a violation of more than 0.5 Å from these restraints are shown in bold. Standard cross-peak: $\gamma CHPro^2$–$\gamma' CHPro^2$ $d = 1.78$ Å.

and of the NMR data collected in the two different solvents strongly suggests that the conformation of the cyclooctapeptide in the two environments is very similar. Consequently, only NMR data obtained in CD_3CN were used for all simulations. The distance restraints were obtained from NOE signals. In addition, coupling-constant restraints were applied as previously reported [13].

The starting structure for all simulations was hand-build using the standard parameters for amino acid residues supplied with the INSIGHT software package. All NMR data were used to determine the backbone conformation. χ_1 dihedral angles of the initial structure were hand-adjusted to values consistent with the $C_\alpha H$–$C_\beta H$ coupling constants and/or NOEs. After this first stage, the cyclic peptide adopted a conformation of high energy. To eliminate artifacts and hot spots a full minimization was performed with NOE restraints and a forcing potential for all peptide bonds of 180°, except for the ω Pro^1–Pro^2 dihedral angle, which was set to 0°. From the minimized structure RMD simulation *in vacuo* at 300 K was performed.

The conformational statistical analysis of the RMD simulation is reported in Table 5, while in Figure 4 the average conformation is shown. The average structure appears quite consistent with all observable NMR NOE effects. A rough estimate of the validity of the proposed structure can be obtained by

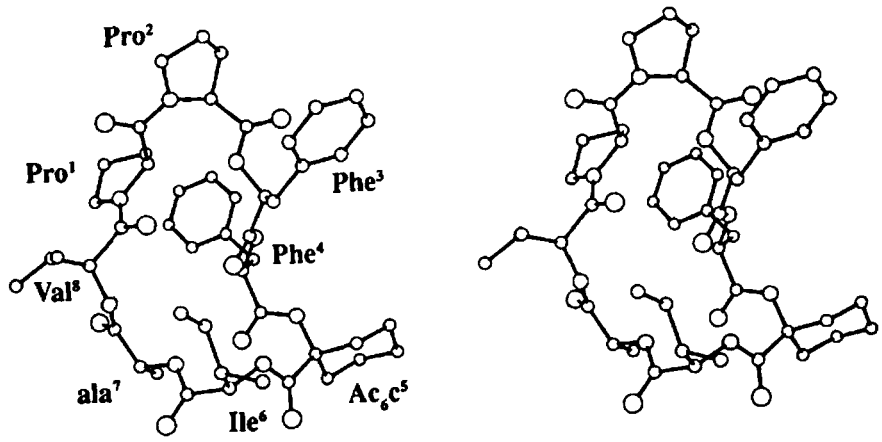

Figure 4 Stereoview of the average structure obtained from RMD simulation *in vacuo* at 300 K.

Table 5 Average Conformational Angles of C8-Ac$_6$c as obtained from the RMD simulation *in vacuo* at 300 K

Residue	ϕ	ψ	ω	χ
Pro^1	− 77.4	157.4	10.1	
Pro^2	− 85.7	28.9	165.5	
Phe^3	− 122.3	79.9	179.6	72.5
Phe^4	− 59.8	− 27.4	171.5	− 83.1
Ac$_6$c^5	− 53.7	− 32.2	168.6	
Ile^6	− 85.0	− 33.6	175.9	− 65.7
ala^7	135.4	− 28.9	170.9	
Val^8	− 110.4	135.0	179.0	− 67.0

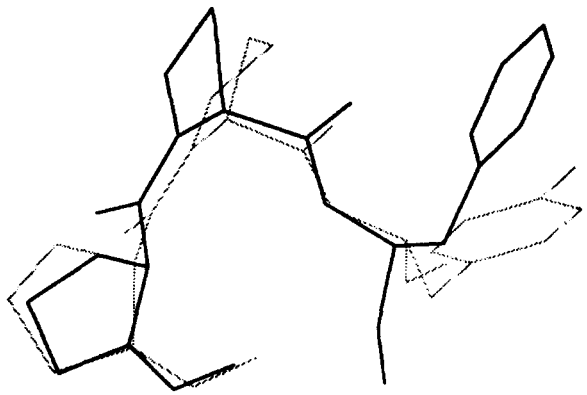

Figure 5 Superimposition of the C8-Ac$_6$c Pro-Pro-Phe moiety (continuous) and Pro-Pro-Tyr segment of hymenistatin 1 (dotted) obtained from [23].

comparing the average RMD structural parameters with the corresponding values derived from the solution conformation of C8-Ac$_6$c, i.e. the corresponding ϕ dihedral angles [45] and the interproton NOE distances. The cyclooctapeptide exhibits one *cis* peptide bond between the Pro^1 and Pro^2 residues, all the others being *trans*. The structure can be described as a *pseudo* β-strand, extending from Pro^2-Ac$_6$c^5 on one side and Ile^6-Pro^1 on the other. The cyclic peptide results stabilized by three well-defined intramolecular H-bonds: a type VIa β-turn about Pro^1-Pro^2 and two consecutive type III β turn between Phe^4-Ac$_6$c^5 and Ac$_6$c^5-Ile^6 residues. The presence of these two consecutive type III β-turns (see Table V) further stabilizes the molecule. In addition, intramolecular H-bonds are found with an occurrence, during the simulation, of 48% between NH group of Val^8 and CO of Phe^3 and of 60% between ala^{7}NH and Phe^{3}CO (C_{13} structure, α-turn). The proposed *pseudo* β-strand conformation is neither flat or extended, but adopts a 'twisted banana' conformation [23]. A careful comparison of the C8-Ac$_6$c structure with conformational parameters of symmetrical and unsymmetrical cyclic octapeptides reveals that our cyclic compound shows significant structural similarity only with hymenistatin 1. In Figure 5 an overlay of the Pro^1-Pro^2-Phe^3 segment of C8-Ac$_6$c with the Pro^1-Pro^2-Tyr^3 moiety of hymenistatin 1 is shown. The conformational parameters proposed for the Pro-Pro-Phe moiety are quite close to those found for the same sequence in the solid-state structures of CLA [3, 7], three analogues of CLA [6, 8–10, 12] and antamanide [46]. Table VI summarizes these structural data. In addition, a further similarity between the structure of C8-Ac$_6$c and those of CLA, CLAIB and antamanide is seen in the Pro^2-Phe^3 sidechain mutual orientation, which produces a similar stacking of the sidechains.

Table 6 Conformational parameters of the Pro-Pro-Phe-Phe Moiety Found in the Solid-state Structures for CLA and its Analogues, Autamanide (AA) and Hymenistatin 1

		Pro[1]	Pro[2]	Phe[3]	Phe[4]
C8-Ac_6c[a]	ϕ	− 77	− 86	− 122	− 60
	ψ	157	29	80	− 27
CLA	ϕ	− 60	− 90	− 97	− 86
[3,7]	ψ	160	− 18	− 49	57
CLAIB	ϕ	− 65	− 90	− 97	− 91
[6,8]	ψ	163	− 17	− 43	58
Tyr^4CLA	ϕ	− 74	− 94	− 97	− 92 (Tyr^4)
[12]	ψ	165	− 5	− 48	62
Cys^5	ϕ	− 70 (Cys^1)	− 95	− 66.5	− 150
[10]	ψ	135	5	− 41	120
Cys^{7a}	ϕ	− 59	− 75	− 87	− 94
[9]	ψ	152	− 32	90	162
AA	ϕ	− 62	− 92	− 101	56
[46]	ψ	160	− 4	− 22	48
Hym1[a]	ϕ	− 63	− 87	− 71 (Tyr^3)	
[3,7]	ψ	144	10	− 61	

The relative references are reported in square brackets.
[a] Average dihedral angles obtained by NMR data.

The RMD average model has been used as the starting structure for a molecular dynamics simulation *in vacuo* at 300 K without constraints. This simulation shows that all trajectories converge to a structure consistent with the NMR data.

The trajectory analysis of ϕ and ψ dihedral angles of all eight residues during the last 20 ps of simulation reveals a low flexibility of the backbone with the highest r.m.s. deviations for the dihedral angles of $\pm 13.0°$. This behaviour differs from that observed for CLA [7] and it is similar to that of CLAIB [8], thus confirming that the introduction of the bulky Ac_6c residue and the reduction of the ring size both contribute to the enhancement of the skeleton rigidity.

CONCLUSIONS

The present study confirms our expectation that in organic solvents at room temperature the reduction of the ring size (from deca- or nona- to octapeptide), coupled with the insertion of sterically hindered helicogenic amino acids and appropriate D-residues, considerably strengthens the molecular rigidity of cyclopeptides.

As far as the overall molecular topology is concerned, the model of the C8-Ac_6c cyclooctapeptide derived from our data shows that:

(1) the conformational behaviour of the molecule is very similar in the two solvents used:
(2) the average structure exhibits structural properties very close to those of the asymmetric hymenistatin 1 cyclooctapeptide.
(3) the 24-membered ring of the eight-residues compound exhibits a 'banana twisted' conformation [23] with a *cis* peptide bond located between the two proline residues. The Pro-Pro-Phe-Phe moiety common to C8-Ac_6c and CLA presents some similar structural features as the stacking between proline and phenylalanine sidechains, even if they appear largely different in their overall solution structure.

In general cyclooctapeptide structures appear quite rigid when compared to related nonapeptides and this behaviour certainly is confirmed in CLA, which in chloroform solution at room temperature exhibits an equilibrium among several conformers [3]. CLA is known to possess specific binding capabilities towards bivalent metal cations [5]. This property has been attributed to the considerable flexibility of the ring, which can appropriately adjust itself in the binding process [5]. In our case no conformational rearrangement seems likely to occur, as is demonstrated by preliminary CD and NMR data, which confirm the absence of any binding specificity in CD_3CN solutions (data not shown).

Acknowledgements

We kindly acknowledge the help of Dr Marco Tatò, Pharmacia Biopharmaceutical, Nerviano, Italy, in carrying out some 2D experiments of the HMBC type. We thank Mr. Marco Mamuccari for technical assistance.

The authors gratefully acknowledge the financial support of the Ministry of Education of Italy (40% and 60%), the C.N.R. and the Human Capital and Mobility Program of the European Community (contract ERBCHRXCT930286).

REFERENCES

1. G. Zanotti, T. Tancredi, F. Rossi, E. Benedetti, C. Pedone and P. A. Temussi (1989). Ala analogues of the cyclolinopeptide A. *Biopolymers 28*, 371–383.
2. T. Tancredi, G. Zanotti, F. Rossi, E Benedetti, C. Pedone and P. A. Temussi (1989). Comparison of the conforma-

tions of cyclolinopeptide A in the solid state and in solution. *Biopolymers 28*, 513–523.

3. B. Di Blasio, F. Rossi, E. Benedetti, V. Pavone, C. Pedone, P. A. Temussi, G. Zanotti and T. Tancredi (1989). Bioactive peptides: solid-state and solution conformation of cyclolinopeptide A. *J. Am. Chem. Soc. 111*, 9089–9098.
4. G. Zanotti, F. Rossi, B. Di Blasio, C. Pedone, E. Benedetti, K. Ziegler and T. Tancredi in: *Peptides: Chemistry, Structure and Biology*, J. E. Rivier and G. R. Marshall, Eds., p. 117–119, ESCOM, Leiden, The Netherlands, 1990.
5. T. Tancredi, E. Benedetti, M. Grimaldi, C. Pedone, F. Rossi, M. Saviano, P. A. Temussi and G. Zanotti (1991). Ion binding of cyclolinopeptide A: an NMR and CD conformational study. *Biopolymers 31*, 761–767.
6. B. Di Blasio, F. Rossi, E. Benedetti, V. Pavone, M. Saviano, C. Pedone, G. Zanotti and T. Tancredi (1992). Bioactive peptides: X-ray and NMR conformational study of [Aib[5,6]-D-Ala[8]] cyclolinopeptide A. *J. Am. Chem. Soc. 114*, 8277–8283.
7. M. Saviano, M. Aida and G. Corongiu (1991). Molecular dynamics simulation *in vacuo* and in solution of cyclolinopeptide A: a conformational study. *Biopolymers 31*, 1017–1024.
8. M. Saviano, F. Rossi, B. Di Blasio, V. Pavone and C. Pedone (1992). Molecular dynamic simulation *in vacuo* and in solution of [Aib[5,6]-D-Ala[8]] cyclolinopeptide A. *J. Biomol. Struct. Dynam. 9*, 1045–1060.
9. G. Zanotti, A. Maione, F. Rossi, M. Saviano, C. Pedone and T. Tancredi (1993). Bioactive peptides: Conformational study of a cystinil cycloheptapeptide in its free and calcium complexed form. *Biopolymers 33*, 1083–1091.
10. F. Rossi, M. Saviano, B. Di Blasio, G. Zanotti, A. Maione, T. Tancredi and C. Pedone (1994). Bioactive peptides: solid state, solution and molecular dynamic studies of a cyclolinopeptide A- related cystinil cyclopentapeptide. *Biopolymers 34*, 273–284.
11. M. Saviano, F. Rossi, M. Filizola, B. Di Blasio and C. Pedone (1995). Structure of [Aib[5,6]-D-Ala[8]] cyclolinopeptide A grown from benzene/acetonitrile mixture. *Acta Cryst. C51*, in press.
12. M. Saviano, F. Rossi, M. Filizola, C. Isernia, B. Di Blasio, E. Benedetti, C. Pedone, I. Z. Siemion and A. Pedyczak (1995). Bioactive peptides: Conformational studies of [Tyr[4]] cyclolinopeptide A. *Biopolymers*, in press.
13. G. Zanotti, F. Rossi, M. Saviano, T. Tancredi, G. Saviano, A. Maione, M. Filizola, B. Di Blasio and C. Pedone (1995). A potent cyclolinopeptide A analogue: solid state and solution conformation of cyclo[Pro-Phe-Phe-Ala-Glu(OtBu)]$_2$. *J. Am. Chem. Soc.*, in press.
14. C. Toniolo and E. Benedetti (1991). Structures of polypeptides from α-amino acids disubstituted at the α-carbon. *Macromolecules 24*, 4004–4009.
15. W. L. Duax, G. D. Smith, C. M. Weeks, V. Z. Pletnev and N. M. Galitsky (1980). An unusual hydrogen bond in type IV β turns of cyclo[(D-Ile-Lac-Ile-D-Hyi)$_2$-]. *Acta Cryst. B36*, 2651–2654.
16. S. Kimura and Y. Imanishi (1983). Synthesis and conformation of the cyclic octapeptides cyclo(Phe-Pro)$_4$, cyclo(Leu-Pro)$_4$ and cyclo(Lys(Z)-Pro)$_4$. *Biopolymers 22*, 2191–2206.
17. T. Shimizu, K. Ueno, Y. Tamaka and K. Tsuda (1983). Ring conformation of cyclic octapeptide cyclo(L-Pro-Sar)$_4$ in the crystalline state. *Int. J. Pept. Protein Res. 22*, 231–238.
18. K. D. Kopple, G. Kartha, K. K. Bhandary and K. Romanowska (1985). Conformations of cyclic octapeptides. 2. Crystal structure of cyclo(D-Ala-Gly-Pro-D-Phe)$_2$. Solvent exposure of backbone protons in crystal and solution conformations. *J. Am. Chem. Soc. 107*, 4893–4897.
19. K. D. Kopple, K. K. Bhandary, G. Kartha, Y. S. Wang and K. N. Parameswaran (1986). Conformations of cyclic octapeptides. 3. Cyclo(D-Ala-Gly-Pro-Phe)$_2$ conformations in crystals and a $T_{1\rho}$ examination of internal mobility in solution. *J. Am. Chem. Soc. 108*, 4637–4642.
20. K. Romanowska and K. D. Kopple (1987). Molecular mechanism investigation of the flexibility of some cyclic peptides. *Int. J. Pept. Protein Res. 30*, 289–298.
21. K. D. Kopple, Y. S. Wang, A. G. Cheng and K. K. Bhandary (1988). Conformations of cyclic octapeptides. 5. Crystal structure of cyclo(Cys-Gly-Pro-Phe)2 and rotating frame relaxation ($T_{1\rho}$) NMR studies of internal mobility in cyclic octapeptides. *J. Am. Chem. Soc. 110*, 4168–4176.
22. D. S. Seetharama Jois, K. R. K. Easwaran, M. Bednarek and E. R. Blout (1992). Conformational and ion binding properties of a cyclic octapeptide, cyclo(Ala-Leu-Pro-Gly)$_2$. *Biopolymers 32*, 993–1001.
23. R. K. Konat, D. F. Mierke, H. Kessler, B. Kutscher, M. Bernd and R. Voegeli (1993). Synthesis and solvent effects on conformation of hymenistatin 1. *Hely. Chim. Acta. 76*, 1649–1666.
24. M. Bodanszky and A. Bodanszky in: *The Practice of Peptide Synthesis*, vol. 21, Springer-Verlag, Berlin 1984.
25. J. P. Tam, W. P. Heath and R. B. Merrifield (1983). SN_2 deprotection of synthetic peptides with a low concentration of HF in dimethyl sulfide: evidence and application in peptide synthesis. *J. Am. Chem. Soc. 105*, 6442–6455.
26. P. Marfey (1984). Determination of D-amino acids. II. Use of bifunctional reagent, 1,5-difluoro-2,4-dinitrobenzene. *Carlsberg Res. Commun. 49*, 591–596.
27. U. Piantini, O. W. Sorensen, R. R. Ernst (1982). Multiple quantum filters elucidating NMR coupling networks. *J. Am. Chem. Soc. 104*, 6800–6801.
28. C. Griesinger, G. Otting, K. Wüthrich and R. R. Ernst (1988). Clean TOCSY for ^{1}H spin system identification in macromolecules. *J. Am. Chem. Soc. 110*, 7870–7872.
29. A. Kumar, R. R. Ernst and K. Wüthrich (1980). A two-

dimensional Overhauser enhancement (2D-NOE) Experiment for the elucidation of complete proton–proton cross-relaxation networks in biological macromolecules. *Biochem. Biophys. Res. Commun. 95*, 1–6.

30. A. A. Bothner-By, R. L. Stephens, J. Lee, C. D. Warren and R. W. Jeanloz (1984). Structure determination of a tetrasaccharide: transient nuclear Overhauser effects in the rotating frame. *J. Am. Chem. Soc. 106*, 811–813.
31. C. Griesinger and R. R. Ernst (1987). Frequency offset effects and their elimination in NMR rotating-frame cross-relaxation spectroscopy. *J. Magn. Reson. 75*, 261–271.
32. A. Bax and S. Subramanian (1986). Sensitivity-enhanced two-dimensional heteronuclear shift correlation NMR spectroscopy. *J. Magn. Reson. 67*, 565–569.
33. A. Bax and M. F. Summers (1986). ^{1}H and ^{13}C assignments from sensitivity-enhanced detection of heteronuclear multiple bond connectivity by 2-D multiple quantum NMR. *J. Am. Chem. Soc. 108*, 2093–2094.
34. H. Kessler, H. Oschkinat, C. Griesinger and W. Bermel (1986). Transformation of homonuclear two-dimensional NMR techniques into one-dimensional techniques using Gaussian pulses. *J. Magn. Reson. 70*, 106–133.
35. Insight/Discover Package, Biosym Technologies, San Diego, CA, USA.
36. S. Lifson, A. T. Hagler and P. Dauber (1979). Consistent force field studies of intermolecular forces in hydrogen-bonded crystals. 1. Carboxylic acids, amides and the C=O···H-hydrogen bonds. *J. Am. Chem. Soc. 101*, 5111–5121.
37. A. T. Hagler, S. Lifson and P. Dauber (1979). Consistent force field studies of intermolecular forces in hydrogen-bonded crystals. 2. A benchmark for the objective comparison of alternative force fields. *J. Am. Chem. Soc. 101*, 5122–5130.
38. A. T. Hagler, P. Dauber and S. Lifson (1979). Consistent force field studies of intermolecular forces in hydrogen-bonded crystals. 3. The C=O···H–hydrogen bond and the analysis of the energetics and packing of carboxylic acids. *J. Am. Chem. Soc. 101*, 5131–5141.
39. L. Verlet (1967). Computer experiments on classical fluids. I. Thermodynamical properties of Lennard-Jones molecules. *Phys. Rev. 159*, 98–103.
40. C. L. Brooks III, B. Montgomery Pettitt, and M. Karplus in: *Proteins: A Theoretical Perspective of Dynamics, Structure and Thermodynamics*, Wiley, New York 1988.
41. K. Wüthrich in: *NMR of Proteins and Nucleic Acids*, Wiley, New York 1986.
42. E. S. Stevens, N. Sugawara, G. M. Bonora and C. Toniolo (1980). Conformational analysis of linear peptides. 3. Temperature dependence of NH chemical shifts in chloroform. *J. Am. Chem. Soc. 102*, 7048–7050
43. O. Convert, H. Duplaa, D. Loeuillet, S. Laville and G. Chassaing (1990). Paramètres RMS utilisés pour la mise en évidence de liaisons hydrogènes dans les peptides. *Analusis 18*, 45–51.
44. J. Fejzo, Z. Zolnai, S. Macura and J. L. Markley (1989). Analysis of laboratory-frame and rotating-frame cross-relaxation buildup rates from macromolecules. *J. Magn. Reson. 82*, 518–528.
45. V. F. Bystrov (1976). Spin–spin coupling and the conformational states of peptide systems. *Progress in NMR Spectroscopy 10*, 41–81.
46. I. L. Karle, T. Wieland, D. Schermer and H. C. J. Ottenheym (1979). Conformation of uncomplexed natural Antamanide-cyrstallized from CH_3CN/H_2O. *Proc. Natl. Acad. Sci. USA 76*, 1532–1536.